Optical Feshbach Resonance Using the Intercombination Transition

K. Enomoto,[1] K. Kasa,[2] M. Kitagawa,[2] and Y. Takahashi[2,3]

[1]*Department of Physics, University of Toyama, 3190 Gofuku, Toyama 930-8555, Japan*
[2]*Department of Physics, Graduate School of Science, Kyoto University, Kyoto 606-8502, Japan*
[3]*CREST, Japan Science and Technology Agency, Kawaguchi, Saitama 332-0012, Japan*

(Received 3 June 2008; published 11 November 2008)

We report control of the scattering wave function by an optical Feshbach resonance effect using ytterbium atoms. The narrow intercombination line ($^1S_0 - {}^3P_1$) is used for efficient control as proposed by Ciuryło *et al.* [Phys. Rev. A **71**, 030701(R) (2005)]. The manipulation of the scattering wave function is monitored with the change of a photoassociation rate caused by another laser. The optical Feshbach resonance is especially efficient for isotopes with large negative scattering lengths such as ^{172}Yb, and we have confirmed that the scattering phase shift divided by the wave number, which gives the scattering length in the zero energy limit, is changed by about 30 nm.

DOI: 10.1103/PhysRevLett.101.203201 PACS numbers: 34.50.Rk, 34.50.Cx, 67.85.Pq, 37.10.De

A magnetically induced Feshbach resonance for tuning the scattering length is a key technique for investigation of quantum degenerate gases of ultracold atoms. Recent realization of superfluidity of fermionic gases is one of the most successful results [1]. This Feshbach resonance occurs when a scattering state in a potential (open channel) is resonantly coupled to a bound state in another potential (closed channel). This resonance modifies the scattering wave function and thus changes the scattering length. Essentially the same phenomenon occurs when laser fields couple a scattering state and a molecular bound state, which is often called an optical Feshbach resonance (OFR) (see Fig. 1) [2–5]. Although this effect causes two-body photoassociation (PA) atom loss due to the spontaneous decay, it has advantages of rapid and localized manipulations. In addition, it is even applicable to atoms for which the magnetic Feshbach resonance is not available. Thus far, the OFR has been demonstrated for alkali-metal atoms by using their dipole-allowed PA transitions [6–8]. In Ref. [6] the modification of the scattering wave function has been observed as the change of a PA transition rate caused by another laser by using a photoionization method. The change of the scattering length has also been measured by Bragg spectroscopy for Bose-Einstein condensates (BECs) with one-color [7] and two-color coupling schemes [8]. However, it has been difficult to change the scattering length by more than about 5 nm in a time scale of 100 μs because of the inevitable severe atom loss and heating.

Recently it has been pointed out that the OFR is quite efficient when a weak intercombination PA transition is employed [9,10]. The narrow linewidth of the intercombination transition allows us to use an excited molecular level close to the dissociation limit, which provides a strong optical coupling because of a large Franck-Condon overlap for the PA transition, while atom loss due to the photon scattering relevant to the atomic resonance is kept small. The OFR is a promising method for controlling the scattering lengths of ytterbium (Yb) and alkaline-earth atoms, which have no hyperfine manifold in the $^1S_0$ ground state and have the $^1S_0 - {}^3P_1$ intercombination transition. The PA spectroscopy of the intercombination transition has been reported for Yb [11,12] and strontium [13].

In this Letter, we have demonstrated the OFR effect using the $^1S_0 - {}^3P_1$ intercombination transition of Yb atoms. The manipulation of the scattering wave function is monitored as the change of the PA atom-loss rate caused by another laser. We have investigated the effect for two isotopes ^{172}Yb and ^{176}Yb, and the result is analyzed with the formalism of Refs. [5,10]. Our result shows that this OFR is especially useful for colliding atom pairs with a large negative scattering length such as ^{172}Yb. We have confirmed that the scattering phase shift divided by the wave number, which gives the scattering length in the zero energy limit, is changed by about 30 nm.

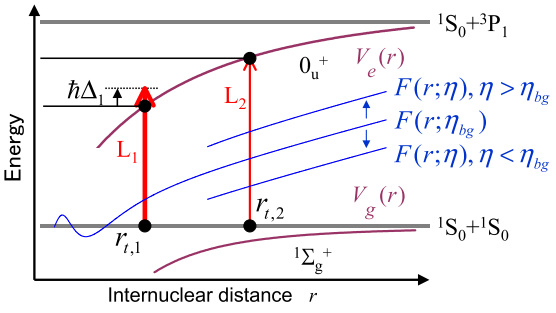

FIG. 1 (color online). Sketch of energy levels, potentials, scattering wave functions, and lasers relevant to this experiment. The frequency of the laser L_1 is tuned near a PA resonance to modify the scattering wave function $F(r;\eta)$ in the ground $^1\Sigma_g^+$ state. In this figure the phase shift η is assumed to be a real value. The frequency of the other laser L_2 is fixed at another PA resonance to monitor the value of $|F(r_{t,2};\eta)|^2$ through the change of its PA rate.

The relevant energy levels and lasers as well as the scattering wave functions are shown schematically in Fig. 1. A scattering state in the ground ${}^1\Sigma_g{}^+$ state connecting to the atomic ${}^1S_0 + {}^1S_0$ state is optically coupled to bound states in the excited 0_u^+ state connecting to the ${}^1S_0 + {}^3P_1$ state. The two lasers are simultaneously introduced to ultracold Yb atoms. One of the lasers (L_1) is intense and its frequency is tuned near a PA resonance to modify the scattering wave function with the OFR effect. The other laser (L_2) is weak and its frequency is fixed at another PA resonance. This laser L_2 is used for monitoring the change of the scattering wave function through the change of its PA rate. Because of the low intensity of the laser L_2, only the laser L_1 is expected to change the scattering wave function.

In the presence of the laser L_1 the scattering matrix element S_{00} for the ground state is given by [5]

$$S_{00} = \exp(2i\eta_{\rm bg})\frac{\Delta_1 - i(\Gamma_1 - \gamma)/2}{\Delta_1 + i(\Gamma_1 + \gamma)/2}, \tag{1}$$

where $\Delta_1 = 2\pi[f_1 - f_0 - \alpha(I_1)] + \epsilon/\hbar$, f_1 is the frequency of L_1, f_0 is the natural frequency of the nearest PA resonance, $\alpha(I_1)$ is the light-induced shift which is a function of the intensity I_1 of L_1, ϵ is the collision energy, and $\hbar$ is Planck's constant divided by 2π. $\eta_{\rm bg}$ is the scattering phase shift in the absence of L_1. $\gamma = 2.29$ MHz [14] is the radiative decay rate of the molecular state, which is twice that of the atomic ${}^3P_1$ state. Γ_1 is the light-induced width given by $\Gamma_1 = 3I_1\gamma\lambda^3 f_{\rm rot} f_{{\rm FC},1}/8\pi c$, where $\lambda = 555.8$ nm is the wavelength of the transition, c is the speed of light, $f_{{\rm FC},1}$ is the Franck-Condon factor per unit energy, and the rotational factor $f_{\rm rot}$ is $1/3$ for the relevant ${}^1\Sigma_g{}^+(J=0) - 0_u^+(J=1)$ transition with J the total angular momentum quantum number. Note that Γ_1 is proportional to the wave number $k = \sqrt{2\mu\epsilon}/\hbar$ for small k, where μ is the reduced mass. A complex phase shift $\eta = \delta + i\zeta$ is extracted from the equation $S_{00} = \exp(2i\eta)$, and the complex scattering length is $-(\delta + i\zeta)/k$ in the limit of $k \to 0$. The real and imaginary parts describe the elastic and inelastic collisions, respectively.

The Franck-Condon factor is calculated under the reflection approximation, which is valid in the present case that the potential $V_e(r)$ in the excited state is much steeper than the potential $V_g(r)$ in the ground state at the internuclear distance $r = r_{t,1}$ [5,10] with $r_{t,1}$ the outer classical turning point of the molecular state photoassociated by L_1. The Franck-Condon factor is then given by $f_{{\rm FC},1} = (dE_{v,1}/dv)|F(r_{t,1};\eta_{\rm bg})|^2/D_1$, where $F(r;\eta_{\rm bg})$ is the scattering wave function in the absence of the laser fields, $dE_{v,1}/dv$ indicates the vibrational spacing, and $D_1 = |\frac{d}{dr}[V_e(r) - V_g(r)]|_{r=r_{t,1}}$. The wave function is asymptotically written as $F(r;\eta_{\rm bg}) = (2\mu/\pi\hbar^2 k)^{1/2}\sin(kr + \eta_{\rm bg})$ at long r. Here we assume that the excited state potential consists of the rather small resonant dipole interaction term and the van der Waals interaction term, that is, $V_e(r) = -C_{3e}/r^3 - C_{6e}/r^6$ with $C_{3e} = 0.194$ a.u. and $C_{6e} = 2.8 \times 10^3$ a.u. [12]. The ground state potential is described as $V_g(r) = -C_{6g}/r^6 - C_{8g}/r^8$ with $C_{6g} = 1.93 \times 10^3$ a.u. and $C_{8g} = 1.9 \times 10^5$ a.u. [15]. The OFR is efficient for the intercombination transition since this Franck-Condon factor is large, even when the detuning-linewidth ratio measured from the atomic resonance is large enough to suppress the photon scattering [9]. Furthermore, as understood from the fact that the wave function $F(r;\eta_{\rm bg})$ is proportional to $r + \eta_{\rm bg}/k$ at long r and for $k = 0$, the Franck-Condon factor and thus Γ_1 at long $r_{t,1}$ become large for large $\eta_{\rm bg}/k$, that is, for a large negative intrinsic scattering length [16]. In this work, we have chosen ^{172}Yb and ^{176}Yb among 5 bosonic isotopes of Yb, since they have large $\eta_{\rm bg}/k$.

In addition, the laser L_1 induces the PA atom loss. The PA rate coefficient $K_{{\rm PA},1}$ due to the laser L_1 is derived from Eq. (1) as [5,10]

$$K_{{\rm PA},1} = \frac{\pi\hbar}{\mu k}\frac{\Gamma_1\gamma}{\Delta_1^2 + (\Gamma_1 + \gamma)^2/4}. \tag{2}$$

The atom loss for a thermal atomic cloud is described as $\dot{n} = -2K_{{\rm PA},1}n^2$ with n the atom density.

The PA rate coefficient $K_{{\rm PA},2}$ due to L_2 is obtained similarly from Eq. (2) by calculating Γ_2 for the modified wave function $F(r;\eta)$, which has the asymptotic form $F(r;\eta) = (2\mu/\pi\hbar^2 k)^{1/2}\sin(kr + \eta)$ at long r. That is, $f_{{\rm FC},2} = (dE_{v,2}/dv)|F(r_{t,2};\eta)|^2/D_2$, and $K_{{\rm PA},2}$ is approximately proportional to $|F(r_{t,2};\eta)|^2$. As shown schematically in Fig. 1, $|F(r_{t,2};\eta)|$ and thus $K_{{\rm PA},2}$ decrease when the real part δ of the phase shift decreases as long as $r_{\rm node} < r_{t,2}$, where $r_{\rm node}$ is the internuclear distance which gives minimum $|F(r;\eta)|$ and corresponds to the last node of the scattering wave function in the $k = 0$ and $\zeta = 0$ case. A clear signature of the modification of the scattering wave function is the *suppression* of the PA atom loss due to the application of the laser L_1. For example, the PA atom loss due to the laser L_2 is almost completely suppressed when $r_{\rm node}$ coincides with $r_{t,2}$. This phenomenon is actually observed in our experiment, when the frequency of the laser L_1 is on the blue-detuning side of the resonance (positive Δ_1).

The experimental setup is almost the same as the previous study of the two-color PA spectroscopy [15]. After Zeeman slowing and a magneto-optical trap, Yb atoms are transferred to a crossed optical trap. The atoms are cooled down to about 1.5 μK with evaporative cooling or sympathetic cooling, and the two lasers L_1 and L_2 are simultaneously introduced to the atoms. These two beams are coupled to the same optical fiber, and are focused on the crossed region of the optical trap. The frequency of L_1 is scanned around a PA resonance at about 800 MHz from the dissociation limit, and the frequency of L_2 is fixed to

another PA resonance at about 300 MHz. The number of remaining atoms is measured by an absorption imaging method. Because of the low temperature of 1.5 μK, only the s-wave scattering is concerned.

In the absence of the lasers, the scattering length and the node position r_{node} are, respectively, $-31.7(3.4)$ and 3.6 nm for ^{172}Yb and are $-1.28(23)$ and 4.0 nm for ^{176}Yb [15]. To achieve the temperature of 1.5 μK for ^{176}Yb atoms, sympathetic cooling with evaporatively cooled ^{174}Yb atoms is performed for about 6 s. For ^{172}Yb the atom loss due to three-body recombination is severe at low temperatures. Therefore the evaporative cooling has to be performed rapidly, for about 1.5 s, to suppress the atom loss.

Figure 2(a) shows the atom-loss spectra for the crossed optical trap region for the ^{172}Yb isotope, which has a large negative scattering length and is expected to show a strong OFR effect. The frequency of L_1 is scanned around a PA resonance at -796 MHz ($r_{t,1} = 6.2$ nm) from the dissociation limit, and the frequency of L_2 is fixed at a PA resonance at -355 MHz ($r_{t,2} = 8.1$ nm). The intensity of the laser L_1 is $I_1 = 1.3$ W/cm^2, corresponding to $\Gamma_1 = 57$ MHz at the collision energy of 1.5 μK. The laser irradiation time is 20 ms. The numbers of atoms without applying the lasers (solid square) and with applying only L_2 (open square) are shown, and they give $\Gamma_2 = 57$ kHz in the absence of L_1.

While the atom-loss spectrum is almost symmetric with respect to the center of the PA signal when only laser L_1 is applied (solid circles), a strongly dispersive spectrum is observed when both lasers L_1 and L_2 are applied (open circles). Figure 2(a) also shows a result of a model calculation with the expected PA atom-loss rates (lines). The PA

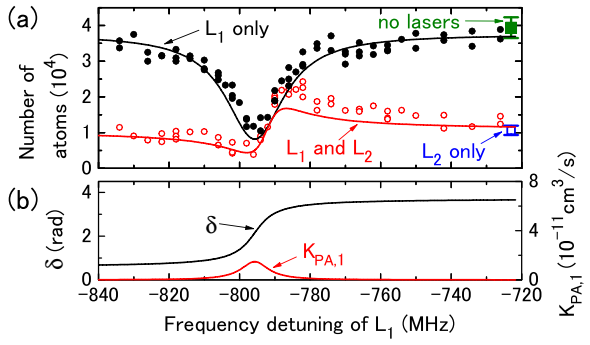

FIG. 2 (color online). (a) Atom-loss spectra for ^{172}Yb with applying only L_1 (solid circles) and with applying both L_1 and L_2 (open circles). The numbers of atoms without applying the lasers and with applying only L_2 are shown as the solid square and the open square, respectively. Their standard deviations are also shown as the error bars. The theoretical spectral profiles are also shown as the lines. The frequency for $\Delta_1 = 0$ is located at -795.7 MHz. (b) Real part δ of the phase shift η and the inelastic collision rate coefficient $K_{\mathrm{PA},1}$ corresponding to the theoretical spectra.

atom loss is described as $\dot{n} = -2K_{\mathrm{PA},1}n^2$ when only L_1 is applied, and is written as $\dot{n} = -2(K_{\mathrm{PA},1} + K_{\mathrm{PA},2})n^2$ when both L_1 and L_2 are applied. These rate equations of the density n are converted to those of the number of atoms by integrating them over the trap volume with assuming a Boltzmann distribution. In this calculation the mean trap frequency is assumed to be 2.7×10^2 Hz, which is within the uncertainty of this experimental parameter. The collision energy is assumed to be 1.5 μK to calculate $K_{\mathrm{PA},1}$ and $K_{\mathrm{PA},2}$. Figure 2(b) shows the corresponding real part δ of the phase shift η and the inelastic collision rate coefficient $K_{\mathrm{PA},1}$. The maximum change of $-\delta/k$ is 68 nm, and the maximum $K_{\mathrm{PA},1}$ is 1.5×10^{-11} cm^3/s, which is about 1 order of magnitude smaller than that for alkali-metal atoms obtained in Ref. [7].

The two experimental spectral profiles shown in Fig. 2(a) come in contact at about -790 MHz. This indicates that $K_{\mathrm{PA},2}$ becomes almost zero at this frequency of L_1 and thus the node position r_{node} of $F(r;\eta)$ becomes equal to $r_{t,2}$. This is consistent with the theoretical result, since theoretical $K_{\mathrm{PA},2}$ becomes also minimum at $\Delta_1/2\pi = 5$ MHz. The corresponding change of $-\delta/k$ is 32 nm.

It should be noted that Γ_1 is much larger than γ in the present case because of the strong optical coupling and the finite temperature: $\Gamma_1 \propto k$ for small k [5]. All the previous experiments of the OFR have not investigated this situation [6–8]. When Δ_1 is scanned through the PA resonance, the real part δ of the phase shift is changed over a range spanning π for $\Gamma_1 > \gamma$ as shown in Fig. 2(b), while it varies dispersively for $\Gamma_1 < \gamma$. It should be emphasized that $K_{\mathrm{PA},1}$ *decreases* with increasing Γ_1 when Γ_1 is much larger than Δ_1 and γ, as understood from Eq. (2) [5,17]. Therefore, a large change of δ/k can be obtained with a small atom-loss rate near the center of the PA resonance in the $\Gamma_1 \gg \gamma$ case. Actually the incomplete atom loss near the PA resonance is observed as shown in Fig. 2(a).

For application to quantum degenerate gases, the atom loss due to the PA and the photon scattering relevant to the atomic resonance have to be small. The photon scattering rate of the laser L_1 for the experimental parameters above is 73 Hz. With a typical atomic density of 10^{13} cm^{-3} and in the $k \to 0$ limit, the above parameters $\Delta_1/2\pi = 5.0$ MHz and $I_1 = 1.3$ W/cm^2 are expected to give a PA atom-loss rate of 4.6×10^2 Hz and to change the scattering length by 68 nm. Therefore, in a submillisecond time scale the scattering length can be changed by tens of nanometers with negligibly small atom loss. While a BEC of ^{172}Yb is unstable because of the large negative scattering length, especially interesting is the case of a polarized fermion-fermion system of ^{171}Yb-^{173}Yb, which has turned out to have a similarly large negative scattering length of $-30.6(3.2)$ nm [15]. Therefore, the OFR is expected to efficiently tune the scattering length of this system. The novel properties of a heteronuclear BCS state using this mixture have been discussed recently [18].

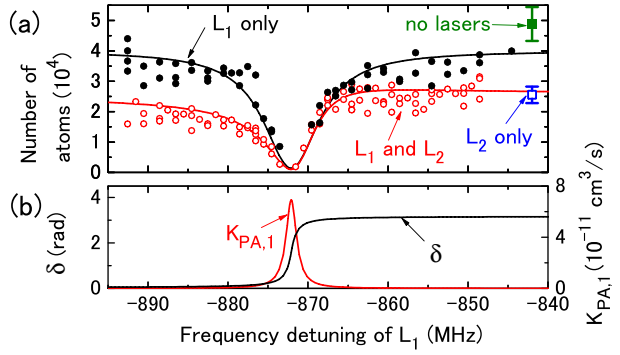

FIG. 3 (color online). (a) Atom-loss spectra for ^{176}Yb with applying only L_1 (solid circles) and with applying both L_1 and L_2 (open circles). The numbers of atoms without applying the lasers and with applying only L_2 are shown as the solid square and the open square, respectively. Their standard deviations are also shown as the error bars. The theoretical spectral profiles are also shown as the lines. The frequency for $\Delta_1 = 0$ is located at -872.1 MHz. (b) Real part δ of the phase shift η and the inelastic collision rate coefficient $K_{\mathrm{PA},1}$ corresponding to the theoretical spectra.

We have also observed the atom-loss spectra of ^{176}Yb, which is shown in Fig. 3(a). The frequency of L_1 is scanned around a PA resonance at about -872 MHz ($r_{t,1} = 6.0$ nm). The frequency of L_2 is fixed at a PA resonance at -260 MHz ($r_{t,2} = 9.0$ nm). The laser intensity is $I_1 = 3.6$ W/cm^2, corresponding to $\Gamma_1 = 7.5$ MHz. The laser irradiation time is 30 ms. This Γ_1 is 1 order of magnitude smaller than that of the case of ^{172}Yb shown in Fig. 2(a), and thus the dispersive behavior of the atom loss is less obvious. Γ_2 is estimated to be 7 kHz from the PA atom loss due to L_2 only. Since the laser L_1 is intense, the photon scattering relevant to the atomic resonance is not negligible and it causes one-body atom decay. The rate β for the one-body atom loss is estimated to be 7 Hz from the tail of the spectrum for which only L_1 is applied. The photon scattering for L_2 is negligible.

Figure 3(a) also shows theoretical atom-loss spectra. Here the one-body loss term $-\beta n$ is added to the rate equations. Assuming that I_1 and Δ_1 are adjusted to give the photon scattering rate of 73 Hz and the PA rate of 4.6×10^2 Hz at $k = 0$ and $n = 10^{13}$ cm^{-3}, which are the same conditions as the above ^{172}Yb case, the change of the scattering length is 12 nm, which is smaller by a factor of about 6 than the change for ^{172}Yb. Figure 3(b) shows the corresponding δ and $K_{\mathrm{PA},1}$. The maximum $K_{\mathrm{PA},1}$ is 6.9×10^{-11} cm^3/s.

In conclusion, we have demonstrated the OFR effect for two bosonic isotopes of Yb using the intercombination transition. The large negative scattering length of ^{172}Yb gives large Γ_1, and thus the OFR becomes very efficient. A straightforward extension of the present work is to apply the OFR to the ^{171}Yb-^{173}Yb fermion-fermion system to generate and to manipulate a heteronuclear BCS state [18]. It is also interesting to generate OFRs using the $^1S_0 - {}^3P_{0,2}$ PA transitions, which have much narrower linewidths than the $^1S_0 - {}^3P_1$ transition and could give a much more efficient OFR effect. These interesting possibilities would benefit the study of various quantum degenerate gases of Yb atoms [19–21], such as dynamics of a BEC with narrow line PA [22].

We thank S. Tojo, H. Hara, A. Yamaguchi, T. Fukuhara, S. Uetake, and Y. Takasu for their help in experiments, and acknowledge P. S. Julienne, P. Naidon, and R. Ciuryło for providing many helpful comments. This work was partially supported by Grant-in-Aid for Scientific Research of JSPS (18204035) and GCOE "The Next Generation of Physics, Spun from Universality and Emergence" from MEXT of Japan.

[1] C. A. Regal *et al.*, Phys. Rev. Lett. **92**, 040403 (2004); M. W. Zwierlein *et al.*, Phys. Rev. Lett. **92**, 120403 (2004); C. Chin *et al.*, Science **305**, 1128 (2004).
[2] P. O. Fedichev, Y. Kagan, G. V. Shlyapnikov, and J. T. M. Walraven, Phys. Rev. Lett. **77**, 2913 (1996).
[3] J. L. Bohn and P. S. Julienne, Phys. Rev. A **56**, 1486 (1997).
[4] R. Napolitano, Phys. Rev. A **57**, 1164 (1998).
[5] J. L. Bohn and P. S. Julienne, Phys. Rev. A **60**, 414 (1999).
[6] F. K. Fatemi, K. M. Jones, and P. D. Lett, Phys. Rev. Lett. **85**, 4462 (2000).
[7] M. Theis *et al.*, Phys. Rev. Lett. **93**, 123001 (2004).
[8] G. Thalhammer, M. Theis, K. Winkler, R. Grimm, and J. H. Denschlag, Phys. Rev. A **71**, 033403 (2005).
[9] R. Ciuryło, E. Tiesinga, and P. S. Julienne, Phys. Rev. A **71**, 030701(R) (2005).
[10] R. Ciuryło, E. Tiesinga, and P. S. Julienne, Phys. Rev. A **74**, 022710 (2006).
[11] S. Tojo *et al.*, Phys. Rev. Lett. **96**, 153201 (2006).
[12] K. Enomoto, M. Kitagawa, S. Tojo, and Y. Takahashi, Phys. Rev. Lett. **100**, 123001 (2008).
[13] T. Zelevinsky *et al.*, Phys. Rev. Lett. **96**, 203201 (2006).
[14] J. E. Golub, Y. S. Bai, and T. W. Mossberg, Phys. Rev. A **37**, 119 (1988).
[15] M. Kitagawa *et al.*, Phys. Rev. A **77**, 012719 (2008).
[16] Properties of scattering wave functions for ultracold collisions are, for example, summarized in a review article [K. M. Jones *et al.*, Rev. Mod. Phys. **78**, 483 (2006)].
[17] M. Junker *et al.*, Phys. Rev. Lett. **101**, 060406 (2008).
[18] D. B. M. Dickerscheid, Y. Kawaguchi, and M. Ueda, Phys. Rev. A **77**, 053605 (2008).
[19] Y. Takasu *et al.*, Phys. Rev. Lett. **91**, 040404 (2003).
[20] T. Fukuhara, Y. Takasu, M. Kumakura, and Y. Takahashi, Phys. Rev. Lett. **98**, 030401 (2007).
[21] T. Fukuhara, S. Sugawa, and Y. Takahashi, Phys. Rev. A **76**, 051604(R) (2007).
[22] P. Naidon, E. Tiesinga, and P. S. Julienne, Phys. Rev. Lett. **100**, 093001 (2008).